Spherical Double Electric Layer Structure and Unprecedented High Stability of the $P_{20}O_{20}$ Cage and Its Anionic Endohedral Complex $Na^-@P_{20}O_{20}$

Yanjin Wang,[†] Jinquan Xu,[‡] Zexing Cao,*[,†] and Qianer Zhang[†]

Department of Chemistry, State Key Laboratory for Physical Chemistry of Solid Surfaces, Center for Theoretical Chemistry, Xiamen University, Xiamen 361005, China, and Department of Chemistry, Quanzhou Normal College, Quanzhou 362000, China

Received: February 8, 2004; In Final Form: March 14, 2004

Density functional calculations are used to determine structures and stabilities of cages P_{20} and $P_{20}O_{20}$ and their endohedral complexes $Na@P_{20}$, $Na^+@P_{20}Na@P_{20}O_{20}$, and $Na^-@P_{20}O_{20}$. Calculations show that the cages P_{20} and $P_{20}O_{20}$ are composed of σ bonds and they have no spherical aromaticity unlike fullerene. Predicted first ionization potential of the endohedral complex $Na@P_{20}$ is 6.04 eV, higher than 5.36 eV of the isolated Na atom. The electron binding energy of the endohedral complex $Na^-@P_{20}O_{20}$ is 6.39 eV, suggesting that $Na@P_{20}O_{20}$ has much higher electron affinity energy than the F atom with the largest elementary electronegativity value. Such outstanding features of the encaged Na species arise from the electrostatic and donor−acceptor interactions between the capsulated species and the cages P_{20} with the σ-bond network and $P_{20}O_{20}$ with the spherical double electric layer. Such novel molecular cages can selectively trap atoms and ions inside and outside, and they may have practical uses as potential building units of nanoscale materials.

In recent years, endohedral cage molecules with atoms and ions inside have received considerable attention[1−17] due to their potential applications as magnetic resonance imaging contrast agents,[19] semiconductors, and ferromagenets.[20] In particular, fullerenes as novel molecular models have been extensively studied both experimentally and theoretically.[1−18] Recently, the smallest fullerene, C_{20}, has been synthesized from its perhydrogenated form $C_{20}H_{20}$ and characterized by photoelectron spectroscopy.[1] Theoretical calculations conclude that the stable I_h-symmetric structure of C_{20} has a charged form of C_{20}^{2+}, which follows the $2(N+1)^2$ rule of spherical aromaticity.[17] At the B3LYP/6-311+G(d, p) level of theory, Moran et al.[5,6] studied equilibrium geometries and stabilities of endohedral complexes $X@C_{20}H_{20}$ (X = H, He, Ne, Ar, Li, Li^+, Be, Be^+, Be^{2+}, Na, Na^+, Mg, Mg^+, and Mg^{2+}). They found that $M@C_{20}H_{20}$ (M=Li, Na, Be, Mg) species possess lower first ionization potential than the Cs atom (3.9 eV): i.e., they are superalkalis.

Like carbon clusters, phosphorus clusters have similarly rich structural variety.[21−25] For example, P_{20} cluster was predicted to have thirteen stable structures by molecular dynamics calculations,[23] even though its most stable isomer depends on methodology.[24,25] However, the endohedral complexes of the phosphorus cluster as a host cage skelecton are fairly less studied until now. In this letter, we present the theoretical exploration on structures and stabilities of the cage clusters P_{20} and $P_{20}O_{20}$ as well as their endohedral complexes. The unprecedented high stability of cage $P_{20}O_{20}$ and dramatic effect of encapsulation on the ionization potential of the capsulated metal species have been discussed.

Geometry optimizations were performed by the B3LYP[26] approach with Los Alamos ECP plus DZ basis set[27] augmented with a *d* polarization function[28] for P, the 3-21G* basis set for Na, and the 3-21G basis set for O atoms, implemented in the Gaussian 98 program.[29] Analytic frequency calculations were used to assess the nature of the stationary structure. Figures 1 and 2 show the equilibrium geometries of the cages P_{20} and $P_{20}O_{20}$ and their endohedral complexes. Relative energies and thermodynamic values (298.15 K) at the B3LYP level of theory are collected in Table 1. Predicted IR spectra of selected stable cages are shown in Figure 3.

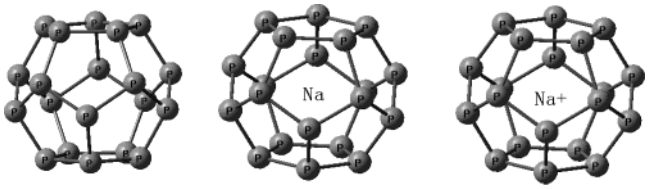

Figure 1. B3LYP optimized structure of cluster P_{20} and its endohedral complexes $Na@P_{20}$ and $Na^+@P_{20}$.

The I_h-symmetric cage of P_{20} comprises twelve pentagons, and the optimized P−P bond length is 2.29 Å, in agreement with 2.29 Å by B3LYP/6-31+G(d)[25b] and 2.24 Å by the MD approach.[23] In contrast to the smallest fullerene C_{20} with the spherical aromaticity,[17,30] the calculated nucleus-independent chemical shift (NICS) at the center of P_{20} is 7.33 ppm by the GIAO method,[31−35] showing that the P_{20} cage has no spherical aromaticity (the negative NICS value, aromaticity; the positive NICS value, antiaromaticity[34]). Natural bond orbital (NBO)[37−42] analyses show that the P_{20} dodecahedron has no π electron systems and the cage in the I_h symmetry actually is composed of P−P σ bonds, and each P vertex has a valence-electron lone pair protruding outward.

The formation of the endohedral complex $Na@P_{20}$ releases energy of 2.50 eV relative to components Na and P_{20}. The P−P bond length in $Na@P_{20}$ is 2.31 Å, slightly longer than the P−P bond length of the isolated P_{20} cage by 0.02 Å. In the endohedral complex, $Na^+@P_{20}$ NBO analyses reveal that the net charge population on Na is +0.72 and notable charge transfer occurs between the metal cation and cage due to the acceptor−donor interaction. The inclusion energy of $Na^+@P_{20}$ is 1.82 eV (Table

* Corresponding author. E-mail: zxcao@xmu.edu.cn. Fax: 86-592-2183047.
[†] Xiamen University.
[‡] Quanzhou Normal College.

10.1021/jp049431k CCC: $27.50
Published on Web 03/20/2004

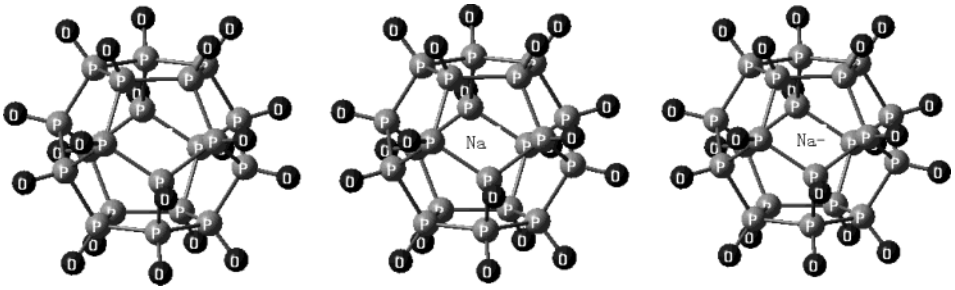

Figure 2. B3LYP optimized structure of cluster $P_{20}O_{20}$ and its endohedral complexes $Na@P_{20}O_{20}$ and $Na^-@P_{20}O_{20}$.

TABLE 1: Relative Energies and Thermodynamic Values (eV) of Cage Clusters P_{20}, $P_{20}O_{20}$, and Their Endohedral Complexes $Na@P_{20}$, $Na^+@P_{20}Na@P_{20}O_{20}$, and $Na^-@P_{20}O_{20}$

process	ΔE^a	$\Delta E + \Delta ZPE$	ΔH	ΔG
$20P \rightarrow P_{20}{}^b$	−2.72	−2.67	−2.69	−2.30
$Na + P_{20} \rightarrow Na@P_{20}$	−2.50	−2.57	2.53	−2.26
$Na^+ + P_{20} \rightarrow Na^+@P_{20}$	−1.82	−1.85	−1.82	−1.47
$P_{20} + 10O_2 \rightarrow P_{20}O_{20}$	−31.28	−30.19	−30.46	−25.68
$P_{20}O_{20} + Na \rightarrow Na@P_{20}O_{20}$	−2.61	−2.71	−2.76	−2.30
$P_{20}O_{20} + Na^- \rightarrow Na^-@P_{20}O_{20}$	−8.49	−8.46	−8.49	−8.11
$Na \rightarrow Na^+ + e^-$	5.36			
$P_{20}Na \rightarrow Na^+@P_{20} + e^-$	6.04	6.09	6.07	6.17
$Na@P_{20}O_{20} + e^- \rightarrow Na^-@P_{20}O_{20}$	−6.39	−6.26	−6.15	−6.31

[a] Relative energies and thermodynamic values are defined by $\Delta F = F_{product} - F_{reactant}$. [b] Values are given in eV/per atom.

1) and the P−P bond length in the cation endohedral cage is 2.31 Å, almost the same as that in $Na@P_{20}$. The calculated first ionization potential of the endohedral complex $Na@P_{20}$ is 6.04 eV, larger than that of the isolated Na atom (5.14 eV by experiment and 5.36 eV by theory). These features of $M@P_{20}$ are different from those of the dodecahedrane endohedral complex $M@C_{20}H_{20}$. Previous studies[5,6] show that the host cage framework of $M@C_{20}H_{20}$ has more compact geometry when the metal atoms, rather than cations, are inside the cage owing to molecular bonding between the encapsulated metal atom and the C−C bonding and C−H antibonding orbitals. Furthermore, the metal-centered $M@C_{20}H_{20}$ behaves as a superalkali.

As Figure 3 displays, the P_{20} cage and its endohedral complexes $Na@P_{20}$ and $Na^+@P_{20}$ are stable structures and they are identifiable by their IR spectra. A slightly geometrical distortion of the framework in $Na@P_{20}$ results in IR spectra that are more complicated than those of P_{20} and $Na^+@P_{20}$ in the I_h symmetry. Relative energies of selected frontier orbitals shown in Figure 4 show that there is an energy level flip between the 3s and 3p orbitals when Na was encapsulated in the P_{20} cage, in comparison with the isolated Na and Na^+. $Na@P_{20}$ has an electron configuration of $\cdots(t_{1u})^1$ ($3p^1$ of Na) in the I_h symmetry and it thus suffers a Jahn−Teller distortion.

On inspection of the data in Table 1, it is clear that the formation of $P_{20}O_{20}$ has huge exothermicity of 31.28 eV with respect to P_{20} and molecular oxygens, showing that the $P_{20}O_{20}$ cage is quite stable. B3LYP calculations predict that the stable $P_{20}O_{20}$ cluster is still in the I_h symmetry, where the P−P and P−O bond lengths are 2.32 Å and 1.53 Å, respectively. The NICS value in the center of the $P_{20}O_{20}$ cage is 6.05 ppm, and thus the host cage of $P_{20}O_{20}$ also has no spherical aromaticity similar to P_{20}. The Na atom was incorporated into the host cage center of $P_{20}O_{20}$, leading to the endohedral complex $Na@P_{20}O_{20}$ with an exothermicity of 2.61 eV. The optimized P−P and P−O bond lengths in $Na@P_{20}O_{20}$ within the I_h symmetry restriction are 2.38 Å and 1.53 Å, respectively. In particular, the inclusion energy of the endohedral complex $Na^-@P_{20}O_{20}$ is 8.49 eV, the highest one among these endohedral complexes. The P−P bond

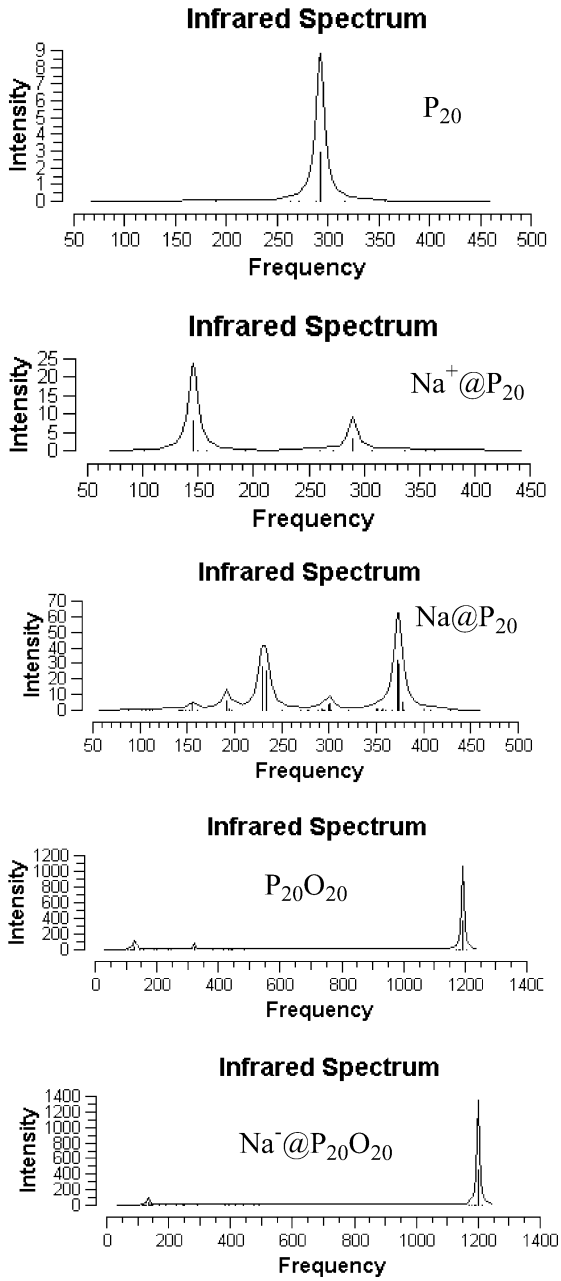

Figure 3. IR spectra of selected stable cages by the B3LYP approach.

length in the anionic complex is 2.32 Å, 0.06 Å shorter than that of the neutral endohedral complex $Na@P_{20}O_{20}$, whereas their P−O bond lengths are almost the same. B3LYP calculations found that the electron affinity energy of the endohedral complex $Na@P_{20}O_{20}$ is 6.39 eV, much higher than that of the F atom (3.40 eV), i.e., the $Na@P_{20}O_{20}$ cage is of superoxidability.

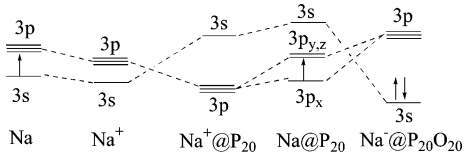

Figure 4. Relative energy levels of (3s, 3p) orbitals of Na.

Frequency analyses show that the stable cages $P_{20}O_{20}$ and $Na^-@P_{20}O_{20}$ have similar IR spectra, while $Na@P_{20}O_{20}$ is not a local minimum on the potential energy surface, where the 5-fold and triply degenerate imaginary frequencies correspond to the inside shift of the encaged Na and the distortion of the cage skelecton, respectively. The $Na@P_{20}O_{20}$ structure in the I_h symmetry has the relative energy level of the frontier orbitals similar to $Na^-@P_{20}O_{20}$ (Figure 4). Therefore, the doublet $Na@P_{20}O_{20}$ does not suffer the Jahn−Teller distortion as seen in $Na@P_{20}$. The unstability of the I_h-symmetric $Na@P_{20}O_{20}$ may arise from strong and complex interactions of the encaged Na with the $P_{20}O_{20}$ double layer structure.

Such striking features of the $M@P_{20}O_{20}$ complexes can be ascribed to the distinct $P^{\delta+}-O^{\delta-}$ double electric layer. Mulliken charge analyses reveal that the Na-centered, P, and O atoms in $Na^-@P_{20}O_{20}$ have charge populations of −0.78, +0.32, and −0.33, respectively. The strongly polarized P−O bonds thus form a spherical double electric layer network. The positively charged inner P shell accommodates the metal anion Na^- and forms the stable complex $Na^-@P_{20}O_{20}$. In addition, strong donor−acceptor interactions, arising from HOMO of Na^- and the antibonding orbital of the P−O bond, result in notable charge transfer between the metal anion and the host cage of $P_{20}O_{20}$. On the other hand, the P atoms bond together through sp^3 hybrid orbitals in cages, and the angle of ∼109 degrees between the bonding orbitals matches the internal angle of 108 degrees of the pentagon very well. The cage of twelve pentagons P_{20} and $P_{20}O_{20}$ suffer thus less strain effect as compared with the I_h-symmetric cage of C_{20} composed of sp^2 carbon atoms. By all appearances, the pentagon should be the favored building unit in the phosphorus cage.

In summary, structures and stabilities of the cages P_{20} and $P_{20}O_{20}$ and their endohedral complexes ($Na@P_{20}$, $Na^+@P_{20}$-$Na@P_{20}O_{20}$, and $Na^-@P_{20}O_{20}$) have been investigated by B3LYP calculations. Present results reveal that the cages P_{20} and $P_{20}O_{20}$ are assembled by σ bonds without extended π-electron systems and they have no spherical aromaticity. In the $P_{20}O_{20}$ cage, the polarized P−O bonds constitute an approximate double electric layer, where the outer O shell is negative and the inner P shell is positive. Such a novel structural model of $P_{20}O_{20}$ can significantly stabilize the capsulated metal anion, which results in that $Na@P_{20}O_{20}$ has much higher electron affinity energy than the F atom. The findings of the present work are helpful for further experimental and theoretical investigations on the endohedral complexes of the host phosphorus clusters.

Acknowledgment. This work was supported by the National Science Foundation of China (Project Nos. 20021002, 20173042 and 20233020) and the Ministry of Education of China.

References and Notes

(1) Prinzbach, H.; Weiler, A.; Landenberger, P.; Wahl, F.; Worth, J.; Scott, L. T.; Gelmont, M.; Olevano, D.; Issendorff, B.v. *Nature* **2000**, *407*, 60.
(2) Weiske, T.; Schwarz, H.; Hirsch, A.; Grosser, T. *Chem. Phys. Lett.* **1992**, *199*, 640.
(3) Rose, H. R.; Dance, I. G.; Fisher, K. J.; Smith, D. R.; Willett, G. D.; Wilson, M. A. *Org. Mass. Spectrom.* **1994**, *29*, 470.
(4) Saunders, M.; Jimenez-Vazquez, H. A.; Cross, R. J.; Mroczkowski, S.; Gross, M. L.; Giblin, D. E.; Poreda, R. J. *J. Am. Chem. Soc.* **1994**, *116*, 2193.
(5) Moran, D.; Woodcock, H. L.; Chen, Z.; Schaefer, H. F.; Schleyer, P. v. R. *J. Am. Chem. Soc.* **2003**, *125*, 11442.
(6) Moran, D.; Stahl, F.; Jemmis, E. D.; Schaefer, H. F., III; Schleyer, P. v. R. *J. Phys. Chem. A* **2002**, *106*, 5144.
(7) Li, Z.; Wei, J.; Zhang, X.; Feng, J. *Chem. J. Chinese Univ.* **1995**, *16*, 256.
(8) Wrackmeyer, B.; Schanz, H. J.; Hofmann, M.; Schleyer, P. v. R. *Angew. Chem., Int. Ed. Engl.* **1998**, *37*, 1245.
(9) Charkin, O. P.; Klimenko, N. M.; Moran, D.; Mebel, A. M.; Charkin, D. O.; Schleyer, P. v. R. *Inorg. Chem.* **2001**, *40*, 6913.
(10) Charkin, O. P.; Klimenko, N. M.; Moran, D.; Mebel, A.; Charkin, D. O.; Schleyer, P. v. R. *J. Phys. Chem. A* **2002**, *106*, 11594.
(11) Moran, D.; Stahl, F.; Jemmis, E. D.; Schaefer, H. F., III; Schleyer, P. v. R. *J. Phys. Chem. A* **2002**, *106*, 5144.
(12) Cioslowski, J. *Electrostatic Structure Calculations on Fullerenes and Their Derivatives*; Oxford University Press: New York, 1995.
(13) *Buckminsterfullerenes*; Billups, W. E.; Ciufolini, M. A., Eds.; VCH Publishers: New York, 1993.
(14) Schleyer, P. v. R.; Najafian, K.; Mebel, A. *Inorg. Chem.* **1998**, *37*, 6765.
(15) Jemmis, E. D.; Balakrishnarajan, M. M. *J. Am. Chem. Soc.* **2000**, *122*, 7392.
(16) Jemmis, E. D.; Jayasree, E. G. *Collect. Czech. Chem. Commun.* **2002**, *67*, 965.
(17) (a) Chen, Z.; Jiao, H.; Moran, D.; Hirsch, A.; Thiel, W.; Schleyer, P. v. R. *J. Phys. Chem. A* **2003**, *107*, 2075. (b) Reiher, M.; Hirsch, A. *Chem. Eur. J.* **2003**, *9*, 5442.
(18) Heath, A. F. *Nature* **1991**, *350*, 600.
(19) Shinohara, H. *Rep. Prog. Phys.* **2000**, *63*, 843.
(20) Irle, S.; Rubin, Y.; Morokuma, K. *J. Phys. Chem. A* **2002**, *106*, 68.
(21) Baudler, M.; Glinka, K. *Chem. Rev.* **1993**, *93*, 1623.
(22) Seifert, G.; Hernandez, E. *Chem. Phys. Lett.* **2000**, *318*, 355.
(23) Bing, S.; Peilin, C. *Phys. Lett.* **2001**, *291*, 343.
(24) Haser, M.; Schneider, U.; Ahlrichs, R. *J. Am. Chem. Soc.* **1992**, *114*, 9551.
(25) (a) Hu, C. H.; Shen, M. Z.; Schadfer, H. F., III *Theor. Chim. Acta* **1992,** *88*, 29. (b) Rulisek, L.; Havlas, Z.; Hermanek, S.; Plesek, J. *Can. J. Chem.* **1998**, 76, 1274.
(26) (a) Beck, A. D. *Phys. Rev. A* **1998**, *38*, 3098. (b) Lee, C.; Yang, W.; Parr, R. G. *Phys. Rev. B.* **1988**, *37*, 785. (c) Beck, A. D. *J. Chem. Phys.* **1993**, *98*, 5648.
(27) Hay, J. P.; Wadt, W. R. *J. Chem. Phys.* **1985**, *82*, 299.
(28) Hollwarth, A.; Bohme, M.; Dapprich, S.; Ehlers, A. W.; Gobbi, A.; Jonas, V.; Kohler, K. F.; Veldkamp, R.; Frenking, G. *Chem. Phys. Lett.* **1993**, *208*, 111.
(29) Frisch, M. J.; Trucks, G. W.; Schlegel, H. B.; Scuseria, G. E.; Robb, M. A.; Cheeseman, J. R.; Zakrzewski, V. G.; Montgomery, J. A., Jr.; Stratmann, R. E.; Burant, J. C.; Dapprich, S.; Millam, J. M.; Daniels, A. D.; Kudin, K. N.; Strain, M. C.; Farkas, O.; Tomasi, J.; Barone, V.; Cossi, M.; Cammi, R.; Mennucci, B.; Pomelli, C.; Adamo, C.; Clifford, S.; Ochterski, J.; Petersson, G. A.; Ayala, P. Y.; Cui, Q.; Morokuma, K.; Malick, D. K.; Rabuck, A. D.; Raghavachari, K.; Foresman, J. B.; Cioslowski, J.; Ortiz, J. V.; Stefanov, B. B.; Liu, G.; Liashenko, A.; Piskorz, P.; Komaromi, I.; Gomperts, R.; Martin, R. L.; Fox, D. J.; Keith, T.; Al-Laham, M. A.; Peng, C. Y.; Nanayakkara, A.; Gonzalez, C.; Challacombe, M.; Gill, P. M. W.; Johnson, B. G.; Chen, W.; Wong, M. W.; Andres, J. L.; Head-Gordon, M.; Replogle, E. S.; Pople, J. A. *Gaussian 98*, revision A.9; Gaussian, Inc.: Pittsburgh, PA, 1998.
(30) Chen, Z.; Jiao, H.; Hirsch, A.; Schelyer, P. v. R. *Angew. Chem, Int. Ed.* **2002**, *41*, 4309.
(31) Wolinski, K.; Hilton, J. F.; Pulay, P. *J. Am. Chem. Soc.* **1990**, *112*, 8251.
(32) Ditchfiels, D. *Mol. Phys.* **1974**, *27*, 789.
(33) McWeeny, R. *Phys. Rev.* **1962**, *126*, 1028.
(34) Dodds, J. L.; McWeeny, R.; Sadlej, A. J. *Mol. Phys.* **1980**, *41*, 1419.
(35) London, F. *J. Phys. Radium, Paris* **1937**, *8*, 1937.
(36) Schelyer, P. v. R.; Maerker, C.; Nicolass, J. R.; Hommes, v. E. *J. Am. Chem. Soc.* **1996**, *118*, 6317.
(37) Carpenter, J. E.; Weinhold, F. *J. Mol. Struct. (THEOCHEM)* **1988** *169*, 41.
(38) Carpenter, J. E.; PhD Thesis, University of Wisconsin, Madison, WI, 1987.
(39) Foster, J. P.; Weinhold, F. *J. Am. Chem. Soc.* **1980**, *102*, 7211.
(40) Reed, A. E.; Weinhold, F. *J. Chem. Phys.* **1983**, *78*, 4066.
(41) Reed, A. E.; Weinstock, R. B.; Weinhold, F. *J. Chem. Phys.* **1985**, *83*, 735.
(42) Reed, A. E.; Curtiss, L. A.; Weinhold, F. *Chem. Rev.* **1988**, *88*, 899.